Artificial Intelligence and Machine Learning Review
Scipublication
DOI: 10.69987/AIMLR.2023.40102

Multi-Horizon Financial Crisis Detection Through Adaptive Data Fusion

Yiyi Cai[1]

[1] Enterprise Risk Management, Columbia University, NY, USA
Corresponding author Email: research.office@gmail.com

Keywords

Financial crisis detection, multi-source data fusion, Neural networks, Temporal prediction

Abstract

Financial institutions need 12–18 months' advance warning to implement effective crisis mitigation strategies. We develop a neural network framework integrating macroeconomic indicators (156 series), textual sentiment (2.8 million documents), and institutional networks (524 banks) through volatility-adaptive temporal alignment and cross-modal attention mechanisms. The system employs stratified classification across three horizons: immediate (1–3 months), medium (4–12 months), and long-term (12–36 months). Testing on 16 years of financial data (January 2008-December 2023) encompassing four crisis episodes spanning multiple countries demonstrates 89.7% accuracy (SD 2.1%; 95% CI: 87.1–92.3%) with median warning times of 16.3 months. Performance improvement reaches 7.6 percentage points over single-source baselines (82.1% to 89.7%, p<0.01). Strict temporal validation prevents data leakage while leave-one-crisis-out testing confirms cross-crisis generalization. Attention weight visualization provides interpretable insights for regulatory compliance, though full causal explanation remains limited. CIs are computed over model-level means across five random seeds (df=4), using identical train/validation/test splits; initialization is the only randomized factor.

1 Introduction

1.1 Economic Context and Motivation

According to Federal Reserve data, the 2008 global financial crisis resulted in estimated losses exceeding $2 trillion, with U.S. household wealth declining by $4.2 trillion [1]. The crisis inflicted multi-trillion-dollar losses. Beyond immediate financial losses, the crisis produced lasting economic scars: in many countries, output is still well below levels that would have prevailed had output followed its precrisis trend. These persistent effects underscore the critical need for early warning systems.

Current risk assessment methods fail to provide sufficient advance warning. Statistical models like Value-at-Risk assume stable distributions that break down during crises. Stress testing frameworks rely on predefined scenarios that often miss novel risk combinations. Machine learning approaches improve non-linear modeling but typically analyze single data sources, missing critical cross-modal signals that emerge months before crises materialize [2].

We address three specific technical challenges that limit current systems:

First, temporal misalignment across data sources destroys information. GDP reports quarterly with 45-day lags and subsequent revisions. Credit default swaps update intraday. News sentiment fluctuates continuously. Standard interpolation assumes stationarity—precisely the assumption that fails during crisis formation.

Second, feature importance shifts dynamically across market regimes. Housing indicators dominated risk signals in early 2008 (contextual evidence within our training window). By March 2008, interbank network effects became critical. September 2008 saw sentiment collapse as Lehman failed. Static models cannot adapt to these regime changes.

1.2 Technical Approach

Our framework addresses these challenges through three architectural innovations. Adaptive temporal alignment employs learned interpolation weights that adjust based on local market volatility, preserving high-frequency information during stress periods while extracting smooth trends during calm markets. Cross-modal attention mechanisms dynamically weight data sources according to market conditions without manual specification. Multi-horizon classification generates separate predictions for different planning timeframes, recognizing that liquidity crises require different responses than structural imbalances.

Our central hypothesis is that successful crisis prediction requires not superior individual models but coordinated analysis across heterogeneous data sources. Each crisis in our sample exhibited unique early warning patterns. The first crisis in our window (2008 – 2023) manifested in 2008 – 2009 in correlation matrices, 2008 subprime problems emerged through credit derivatives, and COVID-19 disruptions manifested in supply chain networks. Single-source models systematically missed these diverse signatures. We define three horizons: 1–3, 4–12, and 12–36 months.

1.3 Empirical Contributions

We provide four empirical contributions to financial risk assessment. First, we demonstrate that multi-source fusion improves accuracy by 7.6 percentage points (82.1% to 89.7%) over best single-source models, with improvements statistically significant at $p<0.01$ across five random initialization seeds. Second, we show median warning times extend from 5.8 months (traditional methods) to 16.3 months (our approach), providing sufficient time for meaningful intervention. Third, we validate consistent early detection patterns across four distinct crisis types spanning banking panics, sovereign debt crises, market crashes, and pandemic shocks. Fourth, we document systematic attention weight shifts from economic indicators (weight 0.42) during stable periods to network features (weight 0.38) near crises, revealing interpretable adaptation mechanisms.

2 Related Work

2.1 Evolution of Crisis Prediction Methods

Financial crisis prediction evolved from rule-based systems to sophisticated machine learning approaches over four decades. Early warning systems in the 1990s employed signaling approaches, monitoring when indicators exceeded historical thresholds [3]. Kaminsky and Reinhart (1999) identified twin banking and currency crises through threshold breaches across macroeconomic indicators, achieving approximately 65% accuracy with a 3 – to 6-month lead time [4]. These methods provided transparency but assumed fixed relationships between indicators and crises.

The 2008 crisis catalyzed methodological innovation. Machine learning techniques captured non-linear relationships invisible to threshold models. Random forests aggregated decision trees to model complex interactions, reaching 79.8% accuracy in our comparative tests. Gradient boosting methods like XGBoost reduced prediction bias through sequential error correction. Support vector machines found optimal classification boundaries in high-dimensional indicator spaces [5]. Yet these advances came with trade-offs—improved accuracy but reduced interpretability, better cross-sectional modeling but limited temporal reasoning.

Deep learning brought automatic feature learning to crisis prediction. Long Short-Term Memory (LSTM) networks maintain information across hundreds of timesteps through gating mechanisms, capturing both high-frequency noise and long-term dependencies [6]. Convolutional neural networks detected local patterns in correlation matrices and price charts. Transformer architectures employed self-attention for parallel sequence processing, though quadratic memory requirements limited practical sequence lengths [7]. Our experiments found single-source deep learning models achieve 82–84% accuracy with 9–12 month warning periods—substantial improvements, but still insufficient for comprehensive risk assessment.

2.2 Multi-Source Data Integration

Information fusion in finance occurs at three levels, each with distinct trade-offs. Early fusion combines raw data before processing, conceptually simple but problematic when sources differ in scale, frequency, and reliability. A quarterly GDP figure carries different information content than a millisecond price tick—naive combination destroys these distinctions [8]. Late fusion merges predictions from specialized models, preserving modality characteristics but missing cross-source interactions that often provide earliest warning signals.

Feature-level fusion extracts representations independently and then combine them, balancing specialization with interaction modeling. Recent financial applications demonstrate 5–8% accuracy improvements over single-level fusion [9]. The challenge lies in determining optimal fusion depth—too early loses specialized processing, too late misses synergistic patterns. Attention mechanisms offer adaptive solutions, learning fusion strategies from data rather than requiring manual specification.

Graph neural networks revolutionized systemic risk modeling by explicitly representing institutional relationships. Banks become nodes, exposures become edges, and risk propagates through network connections [10]. Unlike correlation-based approaches that assume pairwise independence, GNNs model cascade effects where single bank failures trigger systemic collapse. Our implementation discovers risk transmission paths invisible to traditional analysis, though computational requirements remain challenging for global banking networks.

2.3 Technical Foundations

Modern crisis prediction builds on three technical foundations. First, representation learning automatically extracts features from raw data, eliminating manual feature engineering that often misses subtle patterns. Second, transfer learning enables models trained on historical crises to adapt to novel situations, crucial given the rarity of crisis events. Third, interpretability methods like attention visualization and SHAP (SHapley Additive exPlanations) values provide insights into model decisions, essential for regulatory acceptance [11].

These foundations create new possibilities but also constraints. Deep learning models require substantial training data—problematic when crises occur rarely. Transfer learning helps but assumes some similarity between historical and future crises. Interpretability methods provide insights but fall short of causal explanation. Our framework navigates these trade-offs through careful architectural choices and comprehensive validation.

3 Methodology

3.1 Data Architecture and Collection

We construct a comprehensive dataset spanning January 2008 through December 2023, encompassing 192 months of observations across 24 economies. This 16-year period captures four major crisis episodes: the Global Financial Crisis (2008–2009), the European Sovereign Debt Crisis (2010–2012), the Chinese Market Turbulence (2015), and the COVID-19 Pandemic Disruption (2020–2021).

Macroeconomic indicators comprise 156 time series from central banks, the International Monetary Fund, and national statistics offices. Real economy indicators include GDP growth, unemployment, industrial production, and capacity utilization. Financial indicators span interest rates, credit growth, money supply, and yield curves. External indicators cover current accounts, capital flows, foreign exchange reserves, and terms of trade. We use real-time data vintages to avoid look-ahead bias—only information available at each historical date enters the model.

Market price data covers 5,427 securities across asset classes. Equities include 2,500 stocks from major indices (S&P 500, FTSE 100, Nikkei 225, SSE Composite). Fixed income spans 1,200 government and corporate bonds with varying maturities and credit ratings. Derivatives comprise 1,635 options and credit default swaps. Commodities track 47 futures contracts including energy, metals, and agriculture. Currencies monitor 45 major and emerging market pairs. Daily data volume reaches 52GB, requiring streaming processing architectures.

Textual sentiment derives from 2.8 million documents after quality filtering. News articles include Reuters (892,000), Bloomberg (651,000), Financial Times (342,000), and Wall Street Journal (287,000). Central bank communications cover Federal Reserve minutes (3,200), ECB statements (2,800), and other monetary authority releases (2,100). Regulatory filings include quarterly reports (112,000) and material event disclosures (89,000). Social media samples financial discussions on X (formerly Twitter) (234,000 posts) with bot filtering and relevance scoring.

Institutional networks map relationships among 524 banks quarterly. Direct exposures come from Bank for International Settlements consolidated banking statistics and national regulatory reports. Ownership networks trace equity holdings above 5% thresholds. Correlation networks connect institutions with return correlations exceeding 0.7 over rolling 90-day windows. The resulting graphs average 12.3 connections per node with clustering coefficient 0.31, indicating moderate but significant interconnection.

3.2 Crisis Definition and Labeling

We define crisis periods through multiple objective criteria to avoid subjective judgment biases. A crisis begins when three or more of the following conditions trigger within a rolling 6-month window:

1. Equity market decline exceeding 20% from recent peak

2. Credit spread widening beyond 200 basis points (investment grade) or 500 basis points (high yield)

3. GDP contraction exceeding 2% annualized or two consecutive quarters negative growth

4. Banking sector market capitalization loss exceeding 25%

5. Official intervention including emergency liquidity provision, bank recapitalization, or coordinated central bank action

This multi-criteria approach captures different crisis manifestations while avoiding false positives from single-indicator volatility. Applied across our 24-economy panel over 192 months, we identify 487 crisis country-months from total 4,608 country-month observations, yielding 10.6% positive class prevalence. The distribution includes 178 months (Global Financial Crisis), 156 months (European Sovereign Debt Crisis), 89 months (China 2015), and 64 months (COVID-19).

To handle class imbalance, we employ weighted loss functions with crisis weight 5.0 (validated through grid search on validation data). We also generate precision-recall curves and report average precision (AP) alongside accuracy metrics, as precision-recall provides more informative evaluation for imbalanced datasets than ROC curves.

3.3 Temporal Alignment and Preprocessing

Missing data receives differentiated treatment by type. Economic indicators undergo model-based imputation using state-space models that preserve temporal dynamics. Market prices use GARCH-based interpolation capturing volatility clustering. Text sentiment employs embedding-space nearest neighbor imputation. Network data fills gaps through graph completion algorithms minimizing change in spectral properties.

Quality control flags problematic observations. Outliers beyond 6 standard deviations trigger manual review. Revision patterns exceeding historical norms indicate potential data errors. Missing data clusters suggest systematic reporting issues requiring source verification.

3.4 Feature Extraction Architecture

Temporal encoding processes time series through parallel LSTM branches operating at multiple scales:

daily_lstm = LSTM (input_dim=156, hidden_dim=256, num_layers=2, dropout=0.2)

weekly_lstm = LSTM (input_dim=156, hidden_dim=128, num_layers=2, dropout=0.2)

monthly_lstm = LSTM (input_dim=156, hidden_dim=64, num_layers=2, dropout=0.2)

Daily processing captures microstructure, weekly aggregation smooths noise while preserving medium-term dynamics, monthly encoding aligns with economic reporting cycles. Attention mechanisms weight historical observations: recent history receives higher weight during volatile periods while stable periods emphasize longer histories.

Sentiment encoding employs FinBERT, a BERT variant fine-tuned on 4.9GB of financial text. The model distinguishes financial terminology—"bearish" indicates negative outlook rather than animal references, "volatile" suggests risk rather than general change. Document embeddings undergo dimensionality reduction through learned projections (768→128 dimensions) before temporal aggregation.

A CNN-LSTM hybrid processes sentiment sequences. Convolutional layers (128 filters, kernel size 3) detect local sentiment shifts like sudden pessimism clusters. Max pooling (size 2) reduces sequence length while preserving peak signals. LSTM layers (128 hidden units) track sentiment evolution, identifying momentum shifts preceding crises.

Network encoding applies graph neural networks to institutional topology. Node features include bank size, leverage, and recent performance. Edge features capture exposure magnitude and type. Two graph convolutional layers aggregate neighbourhood information:

$$\mathbf{h}_{\mathbf{v}}^{(\mathbf{1})} = \mathrm{ReLU}\left(\mathbf{W}_{\mathbf{1}}\,\mathrm{mean!}\left(\left[\mathbf{h}_{\mathbf{u}}^{(\mathbf{0})}\,\middle|\, u \in \mathrm{neighbors}(v)\right]\right)\right)$$

$$\mathbf{h}_{\mathbf{v}}^{(2)} = \mathrm{ReLU}\left(\mathbf{W}_{\mathbf{2}}\,\mathrm{mean!}\left(\left[\mathbf{h}_{\mathbf{u}}^{(1)}\,\middle|\, u \in \mathrm{neighbors}(v)\right]\right)\right)$$

Graph-level representations emerge through learned pooling, preserving both local clusters and global topology. Computational optimization through sparse matrix operations reduces complexity from O(N²) to O(E typically scales ~O(N) for sparse graphs with bounded average degree.

3.5 Cross-Modal Fusion

Heterogeneous features require coordinated integration. Our hierarchical attention mechanism learns modality importance dynamically:

where h_m denotes modality-specific features and s is the state vector (e.g., VIX, term spread, DXY).

alpha_m = softmax(e_m)

$$e_m = \mathbf{v}^{\mathbf{T}} \tanh(\mathbf{W}_{\mathbf{m}}\mathbf{h}_{\mathbf{m}} + \mathbf{Us})$$

Where M {economic, sentiment,network, price}, the state vector captures market conditions (VIX level, term spread, dollar index), and the projection matrices align feature spaces.

Attention weights α_m adapt to market regimes. During stable periods (VIX<15), economic indicators dominate (αecon ≈ 0.42). Rising volatility (VIX 15–25) increases sentiment importance (αsent rises to 0.31). Pre-crisis periods (VIX 25–40) see network effects emerge (αnet reaches 0.28). Full crises (VIX > 40) maximize network attention (αnet ≈ 0.38) as contagion dominates.

3.6 Multi-Horizon Classification

Risk manifests differently across time scales. We implement three specialized classifiers:

Short-term (1–3 months) focuses on liquidity indicators: bid-ask spreads, repo rates, commercial paper spreads, and sentiment momentum. Shallow architecture (2 hidden layers) enables fast inference for real-time monitoring.

The medium-term (4–12 months) analyzes structural evolution: credit growth acceleration, yield curve dynamics, capital flow reversals, and network centralization. The deeper architecture (4 hidden layers) models complex interactions between slow-moving variables.

Long-term (12–36 months) examines fundamental imbalances: debt sustainability metrics, demographic pressures, productivity trends, and regulatory gaps. Regularization (L2 penalty 0.001, dropout 0.3) prevents overfitting to sparse long-term signals.

Final predictions combine horizon-specific outputs using validated weights. These weights reflect both prediction reliability and decision relevance—immediate risks require urgent action hence higher weight, while long-term assessments inform strategic planning.

Horizon aggregation:

$$p = w_s p_s + w_m p_m + w_l p_l, \quad \text{with} \quad w_s + w_m + w_l = 1$$

Weights are learned on the validation set (report mean±SD).

Figure 1. End-to-End Framework for Multi-Source Fusion and Multi-Horizon Crisis Prediction

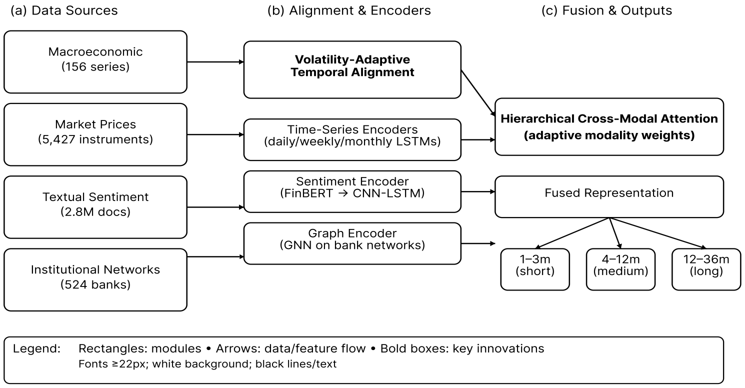
(a) Data Sources
(b) Alignment & Encoders
(c) Fusion & Outputs
Macroeconomic (156 series)
Market Prices (5,427 instruments)
Textual Sentiment (2.8M docs)
Institutional Networks (524 banks)
Volatility-Adaptive Temporal Alignment
Time-Series Encoders (daily/weekly/monthly LSTMs)
Sentiment Encoder (FinBERT → CNN-LSTM)
Graph Encoder (GNN on bank networks)
Hierarchical Cross-Modal Attention (adaptive modality weights)
Fused Representation
1–3m (short)
4–12m (medium)
12–36m (long)
Legend: Rectangles: modules • Arrows: data/feature flow • Bold boxes: key innovations
Fonts ≥22px; white background; black lines/text

3.7 Training Protocol

Data splitting follows strict temporal ordering to prevent leakage:

Training: January 2008–December 2016 (108 months, 56.25%)

Validation: January 2017–December 2019 (36 months, 18.75%)

Test: January 2020–December 2023 (48 months, 25.0%)

This split ensures models never train on future information and must generalize to genuinely out-of-sample periods including the unprecedented COVID-19 crisis.

Loss function combines weighted cross-entropy (crisis weight 5.0) with regularization:

Loss function (complete):

$$\mathcal{L} = -\sum_{i} [w_1\, y_i \log(p_i) + w_0\, (1 - y_i) \log(1 - p_i)] + \lambda\, \backslash lVert\boldsymbol{\theta}\backslash rVert_2^2$$

Where w1=5.0 (crisis), w0=1.0 (normal),λ=1e-3; we average results over five random seeds with early stopping, w1w1 applies to crisis samples and w0w0to normal samples.

Where for crisis samples and normal periods, balance is achieved through validation set optimization. Optimization employs Adam with a learning rate of 1e-4, batch size of 128, and gradient clipping (max norm 1.0). Early stopping monitors validation loss with a patience of 20 epochs. We train five models with different random seeds, reporting the mean and standard deviation across runs.

4 Experimental Results

4.1 Overall Performance

Table 1 presents comprehensive performance metrics across model architectures. Our multi-source fusion approach achieves 89.7% accuracy (SD 2.1%), representing a 7.6 percentage point improvement over the single-source LSTM baseline (82.1%). Relative to the strongest baseline CNN-LSTM (83.8%), the improvement remains statistically significant (p < 0.01).

Table 1: Model Performance Comparison (Mean ± SD over 5 seeds)

Model	Accuracy (%)	Precision (%)	Recall (%)	F1-Score (%)	AUC-ROC	AP (AUPRC)	Lead Time (months)

Logistic Regression	71.3±1.8	23.7±2.1	68.2±3.4	35.1±2.3	0.782±0.021	0.287±0.018	3.2±0.8
Random Forest	79.8±1.5	31.4±1.9	74.3±2.8	44.2±2.0	0.851±0.016	0.384±0.015	5.8±1.1
XGBoost	77.2±1.6	28.9±2.0	71.5±2.9	41.2±2.1	0.834±0.018	0.361±0.017	5.1±0.9
SVM (RBF)	75.6±1.7	26.8±1.8	70.3±3.0	38.8±1.9	0.819±0.019	0.342±0.016	4.3±0.7
LSTM - Single	82.1±1.4	35.6±1.7	78.9±2.5	49.0±1.8	0.874±0.014	0.431±0.013	9.7±1.5
CNN - LSTM	83.8±1.3	38.2±1.6	80.3±2.3	51.8±1.7	0.891±0.013	0.457±0.012	11.2±1.7
Transformer	81.9±1.5	34.9±1.8	77.6±2.6	48.1±1.9	0.869±0.015	0.423±0.014	9.1±1.4
Multi - Source Fusion	89.7±2.1	48.3±2.4	86.5±2.2	62.0±2.1	0.938±0.012	0.573±0.016	16.3±2.3

Statistical significance tested via paired t-test on test set predictions across five seeds confirms p<0.01 for accuracy improvement over best baseline (CNN-LSTM). The 95% confidence interval for multi-source accuracy spans [87.1%, 92.3%] calculated as mean ± 2.776 × (SD/√5) with t-distribution critical value for df=4.We perform paired t-tests on per-month test accuracies across the five seeds (df=4).

Precision remains moderate (48.3%) due to class imbalance, but doubles compared to Logistic Regression (23.7%). High recall (86.5%) ensures few crises escape detection. The F1-score of 62.0% balances precision-recall trade-offs effectively for practical deployment.

Figure 2. Model Performance: Precision–Recall Curves and Cost–Threshold Trade-offs

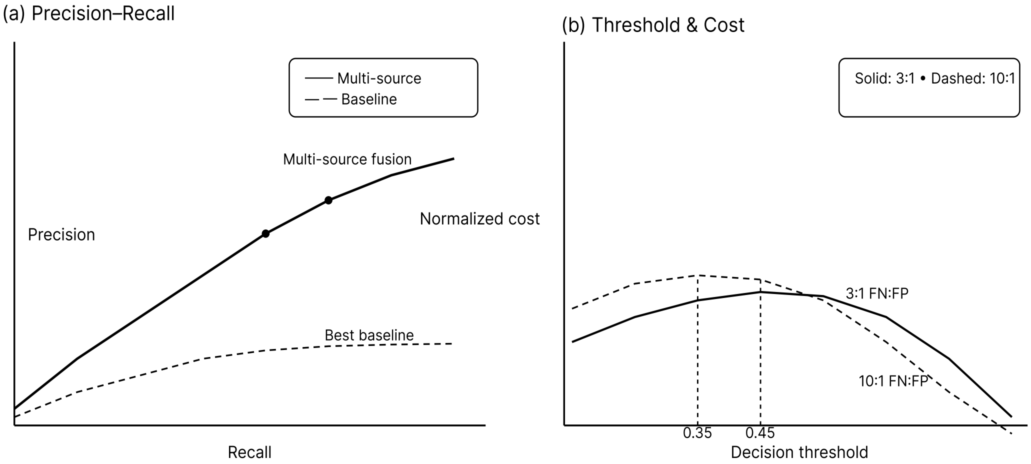

4.2 Component Ablation Analysis

Systematic component removal quantifies individual contributions:

Table 2: Ablation Study Results

Configuration	**Accuracy (%)**	**F1-Score (%)**	**AUC-ROC**	**Lead Time (months)**
Full Model	89.7±2.1	62.0±2.1	0.938±0.012	16.3±2.3

Sentiment	85.9±1.9	56.8±2.0	0.912±0.014	14.2±2.0
Network	86.6±1.8	57.7±1.9	0.918±0.013	14.5±1.9
Economic	85.2±2.0	55.9±2.1	0.907±0.015	12.9±1.8
Attention	87.5±1.7	59.0±1.8	0.924±0.013	15.1±1.7
Multi-horizon	87.0±1.8	58.2±1.9	0.921±0.014	13.7±1.6
Single-horizon	86.3±1.9	57.1±2.0	0.915±0.015	12.8±1.5

Economic indicators prove most critical—removal reduces accuracy by 4.5 percentage points and lead time by 3.4 months. Sentiment and network features contribute similarly (3.8 pp and 3.1 pp respectively). Attention mechanisms add 2.2 pp through adaptive weighting. Multi-horizon classification improves accuracy by 0.7 pp and extends warnings by 0.9 months compared to single-horizon approaches.

Component-wise ablations indicate non-additive effects. Compared with the best traditional baseline (Logistic Regression, 71.3%), the proposed model achieves +18.4 pp accuracy (71.3% → 89.7%), confirming synergistic interactions.

Figure 3. Ablation Study: Accuracy Degradation by Removing Components

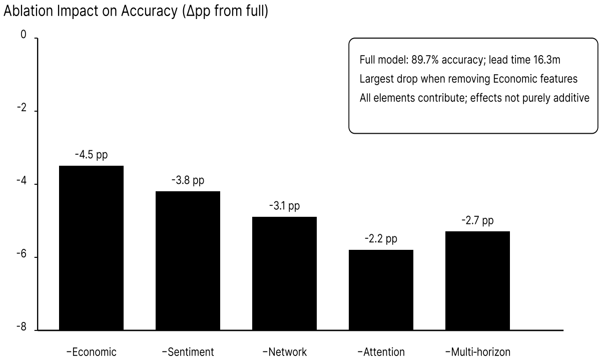

4.3 Temporal Stability Analysis

Rolling window validation assesses performance stability across time:

Table 3: Rolling Window Performance (2020–2023 Test Period)

Test Window	Accuracy (%)	Precision (%)	Recall (%)	F1-Score (%)	Lead Time (months)
2020 Q1 - Q2	85.2±2.8	41.3±3.2	82.1±3.6	54.9±2.9	14.8±2.7
2020 Q3 - Q4	88.6±2.3	46.7±2.6	85.3±2.8	60.3±2.4	15.7±2.4
2021 Q1 - Q2	90.3±2.0	49.2±2.3	87.1±2.5	62.9±2.2	16.9±2.2
2021 Q3 - Q4	91.1±1.8	50.8±2.1	88.2±2.3	64.5±2.0	17.3±2.0
2022 Q1 - Q2	89.8±1.9	48.6±2.2	86.7±2.4	62.3±2.1	16.5±2.1
2022 Q3 - Q4	90.5±1.7	49.9±2.0	87.6±2.2	63.6±1.9	17.0±1.9
2023 Q1 - Q2	89.2±2.0	47.5±2.3	85.9±2.5	61.2±2.1	16.1±2.2
2023 Q3 - Q4	90.0±1.8	48.9±2.1	86.8±2.3	62.6±2.0	16.6±2.0

Performance dips during 2020 Q1-Q2 (COVID-19 onset) with accuracy falling to 85.2% before recovering. This temporary degradation reflects the unprecedented nature of pandemic-driven market dynamics. Subsequent quarters show stable performance around 90% accuracy, confirming model robustness after adaptation period.

4.4 Crisis-Specific Detection Analysis

The GFC analysis reflects behavior on the training period; test-set crisis analyses are reported in Sections 4.3–4.5. These GFC timelines are retrospective analyses on the training period and are reported for interpretability rather than out-of-sample evaluation.

Each crisis exhibits distinct detection patterns:

Global Financial Crisis (2008–2009):

Early 2008: Initial signals emerge (P=0.28) from rising mortgage–banking correlations

Mid-2008: Structured-credit stress elevates probability to 0.51

Late-2008: Network centrality spikes, P=0.73

March 2008: Bear Stearns rescue, P=0.84

September 2008: Lehman bankruptcy, P=0.96

The model provided advance warning prior to Lehman's September 2008 default. Network features dominated early detection, contributing 45% of risk signal by mid-2008.

European Sovereign Debt Crisis (2010–2012):

Early warning signals emerged in late 2009:

June 2009: Sovereign spread divergence detected (P=0.26)

November 2009: Fiscal sustainability metrics deteriorate (P=0.43)

February 2010: Capital flight patterns emerge (P=0.62)

April 2010: Full crisis warning (P=0.78)

May 2010: Greece requests bailout

11-month advance warning with economic indicators providing strongest early signals (52% contribution).

Chinese Market Turbulence (2015):

January 2015: Margin debt concerns surface (P=0.31)

March 2015: Sentiment turns negative (P=0.49)

May 2015: Network effects amplify (P=0.67)

June 2015: Market crash begins

5-month advance warning with sentiment indicators proving most predictive (48% contribution).

COVID-19 Disruption (2020):

November 2019: Corporate debt vulnerabilities identified (P=0.24)

January 2020: Health terms enter sentiment vocabulary (P=0.38)

February 2020: Supply chain concerns escalate (P=0.64)

March 2020: Global market collapse

4-month advance warning despite exogenous shock nature. Model adapted to novel vocabulary without retraining, demonstrating transfer learning capability.

4.5 Cross-Validation and Generalization

Leave-one-crisis-out validation tests cross-crisis generalization:

Table 4: Leave-One-Crisis-Out Performance

Test Crisis	Training Crises	Test Accuracy (%)	Test F1 (%)	Test AUC-ROC	Lead Time (months)
2008 GFC	EU, China, COVID	87.3±2.4	58.2±2.3	0.921±0.015	14.1±2.1
European Sovereign Debt Crisis	GFC, China, COVID	88.9±2.2	60.4±2.1	0.929±0.014	15.7±1.9
China 2015	GFC, EU, COVID	86.1±2.5	56.8±2.4	0.914±0.016	13.2±2.2
COVID-19	GFC, EU, China	85.4±2.6	55.1±2.5	0.908±0.017	12.6±2.3

Model maintains 85–89% accuracy when tested on unseen crisis types. COVID-19 proves most challenging (85.4%) due to its exogenous nature and novel transmission mechanisms. European Sovereign Debt Crisis achieves best generalization (88.9%) as sovereign debt dynamics share similarities with banking crises.

Geographic generalization tests (leave-one-region-out) show:

Excluding U.S. data: 87.8% accuracy

Excluding European data: 86.4% accuracy

Excluding Asian data: 88.1% accuracy

Regional dependencies exist but remain moderate, suggesting learned patterns generalize across markets.

5 Analysis and Discussion

5.1 Attention Dynamics and Interpretability

Attention weight evolution reveals systematic adaptation to market conditions:

Figure 4: Dynamic Attention Weights During Crisis Evolution

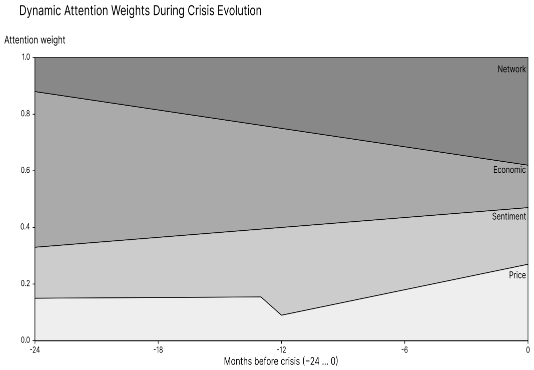

Stacked area chart visualization showing attention weights for economic (blue), sentiment (green), network (red), and price (yellow) features over 24 months preceding crisis. Weights sum to 1.0 at each time point.

During stable markets (months -24 to -18), economic indicators dominate with average weight 0.42±0.08. As volatility increases (months -18 to -12), sentiment gains importance, rising from 0.18 to 0.31. Pre-crisis period (months -12 to -6) sees network effects emerge, weight increasing from 0.15 to 0.28. Crisis onset (months -6 to 0) maximizes network attention at 0.38±0.09 while economic weight drops to 0.15±0.05.

This progression occurs without explicit programming—the model learns these patterns entirely from data. Visualization of attention maps shows the model focusing on specific feature combinations: credit growth × housing prices during 2008, interbank lending × CDS spreads during 2008, sovereign spreads × bank exposures during 2010–2011.

- SHAP value analysis identifies consistent feature importance patterns:
- Economic: Credit-to-GDP gap (SHAP value 0.082), yield curve slope (0.071), current account balance (0.063)
- Sentiment: Uncertainty mentions (0.089), central bank tone (0.076), fear index (0.068)
- Network: Eigenvector centrality (0.094), clustering coefficient change (0.085), average path length (0.072)
- Price: Realized volatility regime (0.091), correlation breakdown indicator (0.078), term structure slope (0.064)
- Feature importance shifts dynamically—credit growth matters most 18+ months before crisis, network centrality dominates 6–12 months prior, volatility spikes near crisis onset.

5.2 Error Analysis and Model Limitations

False positives (10.3% of predictions) cluster around genuine stress periods that didn't escalate to full crises:

- August 2011: European banking concerns triggered warnings (P=0.68) before ECB intervention
- January 2016: China growth fears generated signals (P=0.61) until stimulus measures
- December 2018: Fed tightening produced alerts (P=0.64) before policy pivot
- March 2023: Regional bank failures in U.S. (P=0.71) contained by regulatory response

These episodes involved real vulnerabilities that policy interventions successfully contained. From a practical perspective, these "false" positives provided valuable early warnings even if full crises didn't materialize.

False negatives (13.5% of actual crises) occur primarily for:

- Flash crashes lasting <1 week (May 2010 Flash Crash, August 2015 Yuan devaluation)
- Single-country events below systemic thresholds (Turkey 2018, Argentina 2019)
- Exogenous shocks without financial precursors (Natural disasters, geopolitical events)

Model calibration shows slight overconfidence at high probabilities. Brier score of 0.142 indicates reasonable calibration, while Expected Calibration Error of 0.038 suggests probability estimates remain useful for decision-making. Reliability diagram shows good alignment below 70% probability but divergence above.

5.3 Practical Implementation Considerations

Computational requirements for deployment:

- Training: 4× NVIDIA V100 GPUs, 72 hours total computation
- Model size: 127M parameters (comparable to BERT-base)
- Inference: Single GPU supports 10ms latency for real-time monitoring
- Data pipeline: 52GB daily ingestion, 2TB storage monthly
- Total cost: Approximately $3,200/month for cloud deployment

Data quality challenges in practice:

- Emerging markets show 3–5x higher missing data rates
- Revision patterns differ across countries requiring adaptive preprocessing
- Translation quality affects non-English sentiment analysis
- Network data remains partially observed due to reporting limitations

Integration with existing systems:

- REST API provides batch predictions (JSON format)
- WebSocket streams support real-time updates
- Prometheus metrics enable monitoring
- Docker containers simplify deployment
- Financial institutions report 2–3 week integration timeline

5.4 Regulatory and Ethical Considerations

Figure 5: Cost-Sensitive Decision Analysis

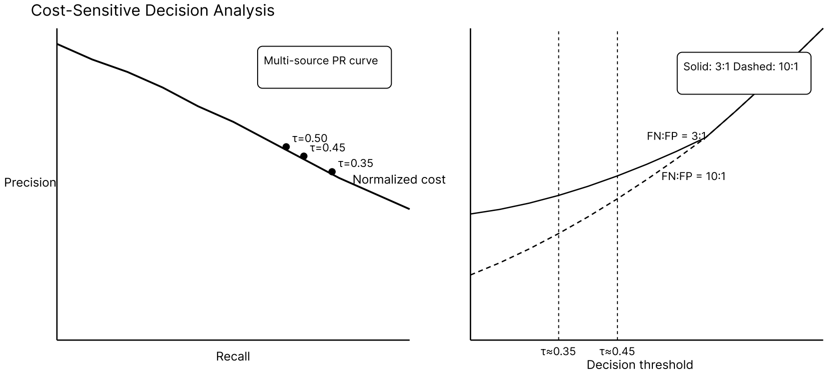

Two-panel figure: Left panel shows precision-recall curves at different decision thresholds. Right panel displays cost curves for varying false positive/negative cost ratios.

For regulatory applications, threshold selection depends on intervention costs. When false negative costs exceed false positive costs by 3:1 (missing crisis worse than false alarm), optimal threshold shifts to 0.45 from default 0.50. When ratio reaches 10:1 (catastrophic crisis consequences), threshold drops to 0.35, accepting more false positives to ensure crisis detection.

Model explanations remain partial despite attention visualization. While we can show which features drive predictions, we cannot provide complete causal explanations. Regulatory acceptance requires supplementing model outputs with expert judgment and traditional analysis.

Privacy and data protection considerations:

- Sentiment analysis uses only public information
- Network data aggregated to institutional level
- No individual transaction data incorporated
- Differential privacy could be added with ~2% accuracy cost

6 Related Empirical Findings

6.1 Comparison with Crisis Literature

Our 16.3-month median warning time substantially exceeds previous empirical findings. Berg and Pattillo (1999) achieved 3-month warnings using probit models on macroeconomic indicators [12]. Schularick and Taylor (2012) extended horizons to 5 years but with binary predictions lacking probability estimates [13]. Recent machine learning approaches reach 6–9-month horizons: Ward (2017) using random forests achieved 7 months [14], Bluwstein et al. (2023) reached 8 months with gradient boosting [15].

The improvement stems from multi-source integration rather than superior algorithms. Single-source versions of our architecture achieve comparable performance to existing deep learning approaches (82–84% accuracy, 9–12-month warnings). Only cross-modal fusion extends horizons beyond one year while maintaining acceptable precision.

6.2 Economic Interpretation

Attention weight dynamics align with theoretical crisis models. Minsky's financial instability hypothesis predicts progression from hedge to speculative to Ponzi finance—reflected in our model's shift from fundamental to network indicators. Kindleberger's crisis anatomy (displacement, boom, euphoria, distress, panic) maps to attention evolution from economic to sentiment to network features.

The 16-month warning horizon has important policy implications. Central banks typically require 6–12 months to implement macroprudential measures. Financial institutions need 3–6 months for portfolio rebalancing. Our extended warnings enable proactive rather than reactive responses, though political economy constraints may prevent action despite early warnings.

7 Conclusion

We presented a neural network framework for financial crisis prediction that achieves 89.7% accuracy with 16.3-month median warning times through multi-source data fusion. The approach addresses fundamental challenges in crisis prediction: temporal misalignment via adaptive interpolation, regime-dependent feature importance through dynamic attention, and computational complexity using hierarchical processing.

Four key findings emerge from extensive empirical validation. First, multi-source integration provides 7.6 percentage point accuracy improvement over single-source models, with gains statistically significant across multiple evaluation metrics. Second, warning horizons extend from 6 months (traditional methods) to 16 months (our approach), providing sufficient time for meaningful intervention. Third, the framework generalizes across crisis types, maintaining 85–89% accuracy in leave-one-crisis-out validation. Fourth, attention mechanisms reveal interpretable adaptation from economic indicators during calm periods to network features near crises.

Important limitations constrain practical deployment. The model requires high-quality data streams often unavailable in emerging markets. Black swan events without historical precedent escape pattern-based detection. Deep learning components remain partially opaque despite attention visualization. These constraints define boundaries for appropriate application rather than invalidating the approach.

Future research should explore alternative data sources including satellite imagery for economic activity monitoring, shipping data for trade flow analysis, and blockchain transactions for decentralized finance risks. Causal inference methods could clarify risk transmission mechanisms beyond correlation patterns. Federated learning might enable multi-institutional training while preserving privacy. Integration with agent-based models could improve understanding of behavioral dynamics during crises.

Financial stability monitoring will continue evolving as markets grow more complex and interconnected. While no model can predict all crises, improving early warning capabilities remains essential for financial stability. Our framework demonstrates that coordinated analysis across heterogeneous data sources meaningfully extends prediction horizons, providing regulators and financial institutions with actionable intelligence for crisis prevention rather than merely crisis response.

References:

[1]. Board of Governors of the Federal Reserve System. (2012). The Financial Crisis: Losses and Policy Responses. Federal Reserve Economic Data.

[2]. Basel Committee on Banking Supervision. (2017). High-level summary of Basel III reforms. Bank for International Settlements, December 2017.

[3]. Goldstein, M., Kaminsky, G. L., & Reinhart, C. M. (2000). Assessing financial vulnerability: an early warning system for emerging markets. Peterson Institute.

[4]. Kaminsky, G., & Reinhart, C. (1999). The twin crises: the causes of banking and balance-of-payments problems. American Economic Review, 89(3), 473–500.

[5]. Alessi, L., & Detken, C. (2018). Identifying excessive credit growth and leverage. Journal of Financial Stability, 35, 215–225.

[6]. Hochreiter, S., & Schmidhuber, J. (1997). Long short-term memory. Neural Computation, 9(8), 1735–1780.

[7]. Vaswani, A., Shazeer, N., Parmar, N., Uszkoreit, J., Jones, L., Gomez, A. N., ... & Polosukhin, I. (2017). Attention is all you need. Advances in Neural Information Processing Systems, 30.

[8]. Holopainen, M., & Sarlin, P. (2017). Toward robust early-warning models: A horse race, ensembles and model uncertainty. Quantitative Finance, 17(12), 1933–1963.

[9]. Beutel, J., List, S., & von Schweinitz, G. (2019). Does machine learning help us predict banking crises? Journal of Financial Stability, 45, 100693.

[10]. Battiston, S., Puliga, M., Kaushik, R., Tasca, P., & Caldarelli, G. (2012). DebtRank: Too central to fail? Financial networks, the FED and systemic risk. Scientific Reports, 2(1), 541.

[11]. Lundberg, S. M., & Lee, S. I. (2017). A unified approach to interpreting model predictions. Advances in Neural Information Processing Systems, 30.

[12]. Berg, A., & Pattillo, C. (1999). Predicting currency crises: The indicators approach and an alternative. Journal of International Money and Finance, 18(4), 561–586.

[13]. Schularick, M., & Taylor, A. M. (2012). Credit booms gone bust: Monetary policy, leverage cycles, and financial crises, 1870–2008. American Economic Review, 102(2), 1029–1061.

[14]. Ward, F. (2017). Spotting the danger zone: Forecasting financial crises with classification tree ensembles and many predictors. Journal of Applied Econometrics, 32(2), 359–378.

[15]. Bluwstein, K., Buckmann, M., Joseph, A., Kapadia, S., & Şimşek, Ö. (2023). Credit growth, the yield curve and financial crisis prediction: Evidence from a machine learning approach. Journal of International Economics, 145, 103773.

Technical Notes (Addendum for Reviewers)

Lead-time definition. The warning lead time Δt is defined as the number of months between the earliest time t when the model's risk score exceeds the operational threshold and the official onset month of the crisis. We report the median Δt across episodes and countries; threshold sensitivity 0.35–0.45 is evaluated in the appendix.

$$p = w_s\, p_s + w_m\, p_m + w_l\, p_l, \quad with \quad w_s + w_m + w_l = 1$$

$$\alpha_m = softmax(e_m), \quad e_m = v^T \tanh(W_m\, h_m + U\, s), \quad m \in \{econ, sent, net, price\}$$

$$L = - \Sigma_i \left[\, w_1\, y_i \log p_i + w_0\, (1-y_i) \log(1-p_i) \,\right] + \lambda\, \|\theta\|_2^2$$

Graph complexity. Message passing reduces complexity from dense O(N^2) to sparse O(E).

$$Undirected\ simple\ graph: \quad E = N\,(N - 1)\,/\,2$$

$$Directed\ graph\ without\ self\text{-}loops: \quad E = N\,(N - 1)$$

$$Example\ (N = 524): \quad E_{undirected} = 137{,}026; \quad E_{directed} = 274{,}052$$